



## Estimating the effect of a phase change material on the performance of a photovoltaic unit using a five parameter model approach

Panagiotis Kladisios, Athina Stegou-Sagia

Laboratory of Heat Transfer and Thermal Processes, School of Mechanical Engineering, National Technical University of Athens, 9 Iroon Polytechniou Str., Zografou 15780, Greece.

Received 19 July 2016; Received in revised form 7 Sep. 2016; Accepted 19 Sep. 2016; Available online 1 March 2017

### Abstract

Photovoltaic modules operate under a large range of conditions. This, combined with the fact that manufacturers provide electrical parameters at specific conditions (STC, Standard Test Conditions) renders the prediction of a PV module's power efficiency very difficult. The most common model for calculating the electric characteristics and, consequently, the generated power of a photovoltaic unit under real transient conditions is the five-parameter model. It is noteworthy that this model demands a relatively small amount of data that are normally available from the manufacturer. The purpose of this paper is to determine the actual benefit in the power efficiency of a photovoltaic unit that has its cell temperature reduced using a phase change material. All approaches of the five-parameter model involve simulating the solar cell, photovoltaic module or photovoltaic array with an one-diode equivalent electrical circuit. The operation of such a circuit is defined by a characteristic I-V equation which contains five parameters: the photocurrent  $I_0$ , the reverse saturation current  $I_s$ , the series resistance  $R_s$ , the parallel resistance  $R_p$  and, depending on the approach, either the diode's ideality factor  $m$  or the modified ideality factor  $\alpha$ . For every pair of cell temperature  $T$  and solar radiation  $G$ , a new characteristic I-V is in effect and, therefore, the above parameters must be calculated anew using correlations between reference and non-reference values of the parameters.

*Copyright © 2017 International Energy and Environment Foundation - All rights reserved.*

**Keywords:** Photovoltaic; Power; Five-parameter model; One-diode equivalent circuit.

### 1. Introduction

A photovoltaic module's generated power depends on the incident solar radiation, the cell temperature and the connected load's resistance. It is common practice for photovoltaic manufacturers to provide the module's nominal power along a minimum set of electrical characteristics such as the maximum power point's current and voltage ( $I_{mp}$  and  $V_{mp}$  respectively), the short circuit current ( $I_{sc}$ ) and the open circuit voltage ( $V_{oc}$ ) under the commonly accepted Standard Test Conditions (STC: cell temperature  $T_{cell}=25$  °C, insolation  $G=1$  kW/m<sup>2</sup>, air mass AM=1.5) [1]. Unfortunately, these conditions rarely occur outside a controlled environment, such as a laboratory, and, therefore, a model that accurately predicts the power efficiency of a module under real, transient conditions is needed. A plethora of models have been proposed with the one-diode and two-diode being the most dominant. The one-diode model has five

unknown parameters, is much simpler to use, and provides an acceptable accuracy. On the other hand, the two-diode model has seven unknown parameters, provides improved accuracy, but its solution is complex due to the implicit form of the current-voltage characteristic equation and the increased sensitivity to the initial guess of the seven parameters [2-8]. Based on the above, the use of a five-parameter model comes as a reasonable choice. The most cited method is proposed by De Soto et al. [9]. Although the theory behind the methodology is sound, it has one major shortcoming: it requires the simultaneous solution of five non-linear equations, a process that can be extremely difficult. Three improved five-parameter methodologies that are based on the one-diode model were investigated as more practical alternatives (M. Paulescu et al., V. Lo Brano et al. and E. Batzelis et al. methodologies) [10-12]. According to the one-diode model, which is also called the standard model, the electrical behaviour of a photovoltaic cell can be modeled with the well known one-diode equivalent electrical circuit shown in Figure 1.

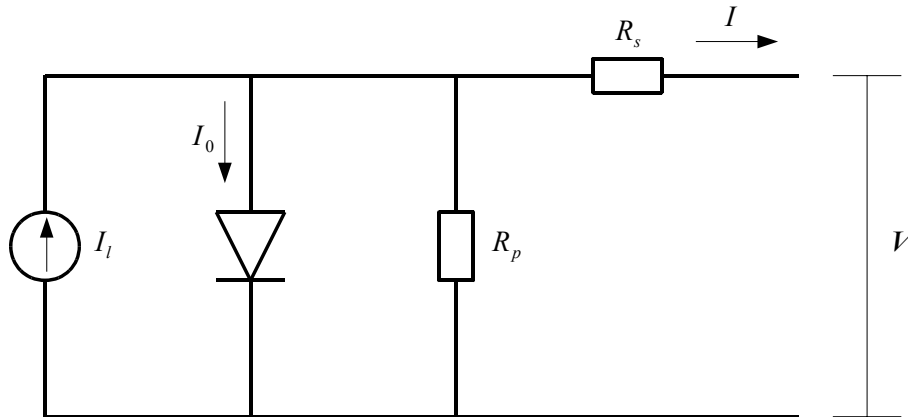


Figure 1. Equivalent one-diode electrical circuit of a solar cell [9].

The equivalent circuit contains a current source that produces the photocurrent ( $I_l$ ), a series resistance ( $R_s$ ), a parallel resistance ( $R_p$ ) and a diode that is characterized by its ideality factor ( $m$ ) and its reverse saturation current ( $I_0$ ). The photocurrent is the current that is generated by the diode when it is exposed to light. It is also proportional to the incident irradiance. Resistances  $R_s$  and  $R_p$  represent the energy and voltage losses that take place in the presence of the photocurrent. The ideality factor is an introduced quantity that determines the deviation from the ideal diode. The reverse saturation current is part of the reverse current in a diode which is caused by diffusion of minority carriers from the neutral regions to the depletion region. This current is almost independent of the reverse voltage [1, 13-17]. The equivalent electrical circuit can be used to simulate an individual solar cell, a photovoltaic module consisting of several cells or a photovoltaic array [9, 13]. Assuming the case of a solar cell and applying Kirchhoff's current law [16, 18, 19]:

$$I = I_l - I_D - I_p \tag{1}$$

where  $I_D$  is the diode current and  $I_p$  is the parallel resistance current. Applying Kirchhoff's voltage law at the right branch which contains the resistances  $R_s$  and  $R_p$ :

$$I_p = \frac{V + IR_s}{R_p} \tag{2}$$

The diode current can be calculated by the Shockley equation [1, 3, 6, 10, 16]:

$$I_D = I_0 \left( e^{\frac{V + IR_s}{mV_t}} - 1 \right) \tag{3}$$

where  $V_t$  is the thermal voltage. The thermal voltage can be calculated by the following equation:

$$V_T = \frac{k_B T}{q} \quad (4)$$

where  $k_B$  is the Boltzmann constant and  $q$  the electron charge. Apparently,  $V_T$  is temperature dependent and at room temperature of 300 K assumes the value of 25.85 mV [16, 17].

Substituting (2), (3) and (4) to (1):

$$I = I_l - I_0 \left( e^{\frac{V+IR_s}{mV_T}} - 1 \right) - \frac{V+IR_s}{R_p} \quad (5)$$

In conclusion, the I-V characteristic equation that describes the solar cell is:

$$I = I_l - I_0 \left( e^{\frac{V+IR_s}{\alpha}} - 1 \right) - \frac{V+IR_s}{R_p} \quad (6)$$

where  $\alpha$  is the modified diode ideality factor:

$$\alpha = \frac{mk_B T}{q} = mV_T \quad (7)$$

Equation (6) can also be used to describe the case of the PV module by converting the five parameters. The equations that relate the values of the parameters between cell and module level are [20]:

$$I_{l,mod} = N_p I_{l,cell} \quad (8)$$

$$I_{0,mod} = N_p I_{0,cell} \quad (9)$$

$$\alpha_{mod} = N_s \alpha_{cell} \quad (10)$$

$$R_{s,mod} = \frac{N_s}{N_p} R_{s,cell} \quad (11)$$

$$R_{p,mod} = \frac{N_s}{N_p} R_{p,cell} \quad (12)$$

where  $N_s$  is the number of solar cells connected in series and  $N_p$  the number of solar cells connected in parallel.

For every distinct pair of cell temperature and insolation, a different I-V characteristic is in effect and, therefore, the five parameters that correspond to these conditions must be calculated. The five-parameter model involves two discrete steps: the calculation of the parameters at STC and the estimation of their values at any operating condition using equations that show the dependence of the parameters between reference and operating conditions [9-12]. The greatest advantage that this specific model provides is that it uses a minimal amount of datasheet information that are normally provided by the manufacturer. Also, the operating point (V,I) of the module lies at the intersection between the characteristic curves of the module and the connected load. Assuming a resistive load  $R_L$  and replacing its characteristic equation into (6), a non-linear equation in terms of I and V is derived. In this paper, this equation was solved numerically using the Newton-Raphson method [21, 22].

The photovoltaic model of choice is Kyocera's KC175GHT, a high efficiency (over 16 %) polycrystalline module [23]. The process of making polycrystalline silicon (p-Si) is much easier and therefore costs less in comparison with other commercial types such as monocrystalline and thin-film panels [24].

In all cases, the proposed methodology was implemented into a Python code.

**2. Mathematical modeling**

*2.1 W. De Soto et al.*

In [9], the most cited methodology is described. The photovoltaic module is described by (6) and, as it was mentioned, the calculation of the parameters at reference and operating conditions is required.

*2.1.1 Five parameters at STC*

In order to extract the five parameters at the reference conditions, five equations are needed [9, 20]. According to W. De Soto et al., three known I-V pairs are substituted into (6), which describes the photovoltaic module.

Short circuit point:

$$I_{sc,ref} = I_{l,ref} - I_{0,ref} \left[ e^{\frac{I_{sc,ref} R_{s,ref}}{a_{ref}}} - 1 \right] - \frac{I_{sc,ref} R_{s,ref}}{R_{p,ref}} \tag{13}$$

Open circuit point:

$$0 = I_{l,ref} - I_{0,ref} \left[ e^{\frac{V_{oc,ref}}{a_{ref}}} \right] - \frac{V_{oc,ref}}{R_{p,ref}} \tag{14}$$

Maximum power point:

$$I_{mp,ref} = I_{l,ref} - I_{0,ref} \left[ e^{\frac{V_{mp,ref} + I_{mp,ref} R_{s,ref}}{a_{ref}}} - 1 \right] - \frac{V_{mp,ref} + I_{mp,ref} R_{s,ref}}{R_{p,ref}} \tag{15}$$

Observing that the derivative of power P with respect to V at the maximum power point equals to zero, a fourth equation is derived:

$$\left. \frac{d(P)}{dV} \right|_{mp} = I_{mp} + V_{mp} \left. \frac{dI}{dV} \right|_{mp} = 0 \rightarrow \frac{-\frac{I_{0,ref}}{a_{ref}} e^{\frac{V_{mp,ref} + I_{mp,ref} R_{s,ref}}{a_{ref}}} - \frac{1}{R_{p,ref}}}{1 + R_{s,ref} \left( \frac{I_{0,ref}}{a_{ref}} e^{\frac{V_{mp,ref} + I_{mp,ref} R_{s,ref}}{a_{ref}}} + \frac{1}{R_{p,ref}} \right)} = -\frac{I_{mp,ref}}{V_{mp,ref}} \tag{16}$$

The fifth equation that completes the system exploits the linear dependence of the open circuit voltage to temperature:

$$\mu_{Voc} = \left. \frac{\partial V}{\partial T} \right|_{oc} \approx \frac{V_{oc,T} - V_{oc,ref}}{T - T_{ref}} \tag{17}$$

where T is a cell temperature near the reference temperature and  $\mu_{Voc}$  is open circuit temperature coefficient. Expression (17) combined with the dependence equations of the following section, lead to another open circuit point equation:

$$0 = I_{l,T} - I_{0,T} \left( e^{\frac{V_{oc,T}}{a_T}} - 1 \right) - \frac{V_{oc,T}}{R_{p,T}} \tag{18}$$

In [25] W. De Soto proposed an alternative approach for the fifth equation that is appropriate when the open circuit temperature coefficient  $\mu_{Voc}$  is not provided by the manufacturer. The slope of the characteristic curve near the short circuit point is almost horizontal and dependent on the parallel resistance:

$$\left. \frac{dI}{dV} \right|_{sc} = -\frac{1}{R_{p,ref}} = 0 \rightarrow \frac{-\frac{I_{0,ref}}{a_{ref}} e^{\frac{I_{sc,ref} R_{s,ref}}{a_{ref}}} - \frac{1}{R_{p,ref}}}{1 + R_{s,ref} \left( \frac{I_{0,ref}}{a_{ref}} e^{\frac{I_{sc,ref} R_{s,ref}}{a_{ref}}} + \frac{1}{R_{p,ref}} \right)} = -\frac{1}{R_{p,ref}} \quad (19)$$

Therefore, a system of five non-linear equations with five unknowns that consists of (13)-(16) and either (18) or (19) must be solved in order to extract the reference parameters. The simultaneous solution of five non-linear equations can be solved with the Newton-Raphson method. However, this method requires the calculation of the system's Jacobian matrix. The calculation of a large amount of partial derivatives, many of which have complex expressions, is evidently impractical. Attempts to solve the system with the simpler Gauss-Seidel method and Python's fsolve (scipy module) were faced with initialization and convergence difficulties and, therefore, were inconclusive [21, 22]. For the above reason, more practical alternatives were investigated.

### 2.1.2 Five parameters outside STC

In [9] the following set of equations is proposed for the dependence of the parameters on reference conditions:

-Modified ideality factor

$$\frac{a}{a_{ref}} = \frac{T}{T_{ref}} \rightarrow m = m_{ref} \quad (20)$$

-Reverse saturation current

$$\frac{I_0}{I_{0,ref}} = \left( \frac{T}{T_{ref}} \right)^3 e^{\left[ \frac{1}{k_B} \left( \frac{E_{g,ref}}{T_{ref}} - \frac{E_g}{T} \right) \right]} \quad (21)$$

where  $E_g$  is the bandgap energy. For silicon, at reference temperature  $E_{g,ref}=1.121$  eV.  $E_g$  in other temperatures can be calculated by:

$$\frac{E_g}{E_{g,ref}} = 1 - 0.0002677(T - T_{ref}) \quad (22)$$

-Photocurrent

$$I_l = \frac{G}{G_{ref}} [I_{l,ref} + \mu_{Isc}(T - T_{ref})] \quad (23)$$

where  $\mu_{Isc}$  is the short circuit temperature coefficient and  $G$ ,  $G_{ref}$  are the insolation and reference insolation.

-Parallel resistance

$$\frac{R_p}{R_{p,ref}} = \frac{G_{ref}}{G} \quad (24)$$

-Series resistance

$$R_s = R_{s,ref} \quad (25)$$

2.2 V. Lo Brano et al.

Another frequently cited approach is described at [10]. According to V. Lo Brano et al., a new variation of (6) is proposed to describe the PV module:

$$I = \alpha_G I_t - I_0 \left( e^{\frac{\alpha_G [V + KI(T - T_{ref})] + IR_s}{a_G m T}} - 1 \right) - \frac{\alpha_G [V + KI(T - T_{ref})] + IR_s}{R_p} \tag{26}$$

where  $\alpha_G$  is the ratio between the actual incident insolation and the reference insolation and K the thermal correction factor.  $\alpha_G$  is calculated by (27) and K by (28):

$$\alpha_G = G / G_{ref} \tag{27}$$

$$K = \frac{V_{mp} - V_{mp}^*}{I_{mp}^* (T^* - T_{ref})} \tag{28}$$

$V_{mp}^*$  and  $I_{mp}^*$  are the maximum power point voltage and current under cell temperature  $T^*$ , other than  $T_{ref}$  (usually 75 °C), and solar radiation  $G=1kW/m^2$ . These values are extracted by either tabular or graphical data procured by the manufacturer.  $V_{mp}$  is the maximum power point voltage that is calculated by (26) for  $K=0$ . In [10], one of the tested models matches the electrical characteristics of the PV model chosen for this paper. For simplicity the following value, already calculated in [10], was assumed:

$$K = 0.0012 \left[ \frac{\Omega}{^\circ C} \right]$$

From [23], the following Table 1 is extracted:

Table 1. Electrical characteristics under standard test conditions.

Electrical characteristics under STC (T=25 °C, G=1000 W/m <sup>2</sup> , AM=1.5)					
$V_{mp,ref}$ [V]	$I_{mp,ref}$ [A]	$V_{oc,ref}$ [V]	$I_{sc,ref}$ [A]	$\mu_{V,oc,ref}$ [V / °C]	$\mu_{I,sc,ref}$ [A / °C]
23.6	7.42	29.2	8.09	-0.109	0.00318

The V. Lo Brano et al. approach, much like in the case of W. De Soto et al., involves two parts: The calculation of the five parameters at STC using an iterative algorithm and the calculation of the five parameters at operating conditions using dependence equations between reference and operating values.

2.2.1 Five parameters at STC

The five parameters at STC will be calculated by a system five equations using an iterative algorithm. The system is a product of the I-V characteristic at STC. The three distinct points of the curve (short circuit, open circuit, maximum power) give the following equations:

-Short circuit point (V=0, I=I<sub>sc</sub>):

$$I_{sc,ref} = I_{l,ref} - I_{0,ref} \left( e^{\frac{I_{sc,ref} R_{s,ref}}{m_{ref} T_{ref}}} - 1 \right) - \frac{I_{sc,ref} R_{s,ref}}{R_{p,ref}} \tag{29}$$

-derivative at short circuit point:

$$\left. \frac{dI}{dV} \right|_{V=0, I=I_{sc,ref}} = - \frac{\frac{I_{0,ref}}{m_{ref} T_{ref}} e^{\frac{I_{sc,ref} R_{s,ref}}{m_{ref} T_{ref}}} + \frac{1}{R_{p,ref}}}{1 + R_{s,ref} \left( \frac{I_{0,ref}}{m_{ref} T_{ref}} e^{\frac{I_{sc,ref} R_{s,ref}}{m_{ref} T_{ref}}} + \frac{1}{R_{p,ref}} \right)} = - \frac{1}{R_{po}} \tag{30}$$

-open circuit point ( $V=V_{oc}$ ,  $I=0$ ):

$$0 = I_{l,ref} - I_{0,ref} \left( e^{\frac{V_{oc,ref}}{m_{ref}T_{ref}}} - 1 \right) - \frac{V_{oc,ref}}{R_{p,ref}} \quad (31)$$

-derivative at open circuit point:

$$\left. \frac{dI}{dV} \right|_{V=V_{oc,ref}, I=0} = - \frac{\frac{I_{0,ref}}{m_{ref}T_{ref}} e^{\frac{V_{oc,ref}}{m_{ref}T_{ref}}} + \frac{1}{R_{p,ref}}}{1 + R_{s,ref} \left( \frac{I_{0,ref}}{m_{ref}T_{ref}} e^{\frac{V_{oc,ref}}{m_{ref}T_{ref}}} + \frac{1}{R_{p,ref}} \right)} = - \frac{1}{R_{so}} \quad (32)$$

-maximum power point:

$$I_{mp,ref} = I_{l,ref} - I_{0,ref} \left( e^{\frac{V_{mp,ref} + I_{mp,ref}R_{s,ref}}{m_{ref}T_{ref}}} - 1 \right) + \frac{V_{mp,ref} + I_{mp,ref}R_{s,ref}}{R_{p,ref}} \quad (33)$$

The quantities  $R_{po}$ ,  $R_{so}$ , are, apparently, the reciprocals of the slope of the characteristic curve at the short circuit and open circuit point respectively [10]. Using the provided characteristic curve we get Figure 2. The above result in the following estimations of  $R_{po}$  and  $R_{so}$ :

$$R_{po} = 100\Omega$$

$$R_{so} = 0.04\Omega$$

Solving (29), (30), (31), (32), (33) for  $I_{l,ref}$ ,  $R_{p,ref}$ ,  $m_{ref}$ ,  $R_s$ ,  $I_{0,ref}$  respectively:

$$I_{l,ref} = I_{sc,ref} + I_{0,ref} \left( e^{\frac{I_{sc,ref}R_{s,ref}}{m_{ref}T_{ref}}} - 1 \right) + \frac{I_{sc,ref}R_{s,ref}}{R_{p,ref}} \quad (34)$$

$$R_{p,ref} = \frac{R_{po} - R_{s,ref}}{1 - \left( R_{po} - R_{s,ref} \right) \frac{I_{0,ref}}{m_{ref}T_{ref}} e^{\frac{I_{sc,ref}R_{s,ref}}{m_{ref}T_{ref}}}} \quad (35)$$

$$m_{ref} = \frac{V_{oc,ref}}{T_{ref} \ln \left( \frac{I_{l,ref} + I_{0,ref} - \frac{V_{oc,ref}}{R_{p,ref}}}{I_{0,ref}} \right)} \quad (36)$$

$$R_{s,ref} = \frac{\left[ \left( \frac{I_{0,ref}}{m_{ref}T_{ref}} \right) e^{\frac{V_{oc,ref}}{m_{ref}T_{ref}}} + \frac{1}{R_{p,ref}} \right] R_{so} - 1}{\left[ \left( \frac{I_{0,ref}}{m_{ref}T_{ref}} \right) e^{\frac{V_{oc,ref}}{m_{ref}T_{ref}}} + \frac{1}{R_{p,ref}} \right]} \quad (37)$$

$$I_{0,ref} = \frac{I_{l,ref} - I_{mp,ref} - \frac{V_{mp,ref} + I_{mp,ref}R_{s,ref}}{R_{p,ref}}}{e^{\frac{V_{mp,ref} + I_{mp,ref}R_{s,ref}}{m_{ref}T_{ref}}} - 1} \quad (38)$$

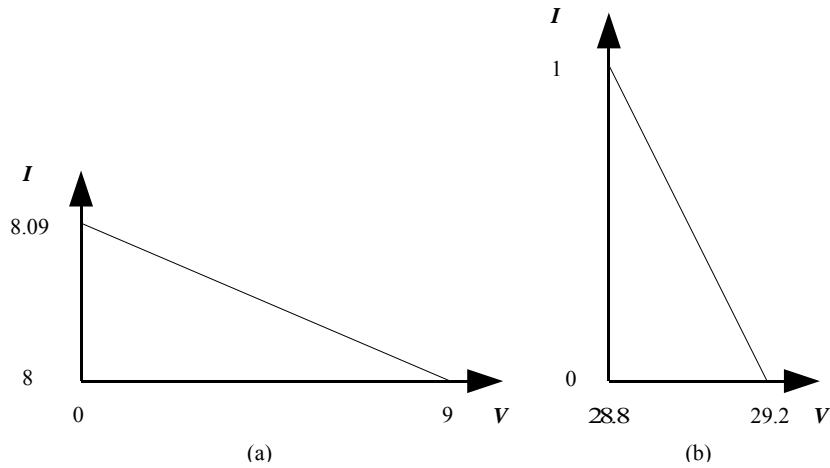


Figure 2. Graphical estimation of  $R_{p0}$  at the short circuit point (a) and of  $R_{s0}$  at the open circuit point (b).

In the present methodology an iterative algorithm is proposed to solve the above system of five non-linear equations (34-38). Its flow chart is depicted in Figure 3 (a). Using initial guess values for  $m_{ref}$  and  $R_{s,ref}$  and the initial conditions  $I_{l,ref}=I_{sc,ref}$ ,  $R_p=R_{p0}$ , the reverse saturation current  $I_{0,ref}$ , the photocurrent  $I_{l,ref}$  and the parallel resistance  $R_{p,ref}$  are calculated using (38), (34) and (35) respectively. With  $I_{0,ref}$ ,  $I_{l,ref}$ ,  $R_s$  and  $R_p$ , known,  $m_{ref}$  is recalculated using (36). This process is repeated until the desirable accuracy is reached. After convergence,  $R_{s,ref}$  is recalculated using (37). The new  $m_{ref}$ ,  $R_{s,ref}$  are in turn used, repeating all of the above until the convergence of  $R_{s,ref}$  is achieved. The proposed algorithm is actually two trial and error processes with one of them nested inside the other.

The above procedure resulted into the values of the five reference parameters:

$$\begin{aligned}
 I_{l,ref} &= 8.1084 [A] \\
 I_{0,ref} &= 3.4403 \cdot 10^{-9} [A] \\
 m_{ref} &= 0.0045 \left[ \frac{V}{K} \right] \\
 R_{s,ref} &= 0.2269 [\Omega] \\
 R_{p,ref} &= 99.7732 [\Omega]
 \end{aligned}$$

### 2.2.2 Five parameters outside STC

According to [7] some parameters may be considered to be constant, a hypothesis that will render the proposed model simpler but, at the same time, inaccurate in cases of partial shading. Presently,  $m$ ,  $R_s$ ,  $R_p$  are assumed to be constant [10]. It should be noted that,  $m$  and  $R_s$  are affected by cell temperature at a negligible degree [26].

$$m = m_{ref} \tag{39}$$

$$R_s = R_{s,ref} \tag{40}$$

$$R_p = R_{p,ref} \tag{41}$$

with  $m$ ,  $R_s$ ,  $R_p$  remaining unaltered, a correlation between  $I_{l,ref}$ ,  $I_{0,ref}$  and  $I_l$ ,  $I_0$  remains.  $I_l$  can be immediately calculated by the following equation:

$$I_l = I_{l,ref} + \mu_{isc} (T - T_{ref}) \tag{42}$$

where  $\mu_{isc}$  the short circuit temperature coefficient.

A good approximation of  $I_0$  can be achieved with:

$$I_0 = e^{\frac{a_G - 0.2}{1.0 - 0.2} \ln \frac{I_0(1,T)}{I_0(0.2,T)} + \ln I_0(0.2,T)} \tag{43}$$



$I_0(1,T)$  and  $I_0(0.2,T)$  are the reverse saturation currents for cell temperature  $T$  and solar radiation ratios 1 and 0.2 respectively.  $I_0(1,T)$  and  $I_0(0.2,T)$  can be calculated from (44):

$$I_0 = a_G \frac{I_l - \frac{V_{oc}(a_G, T)}{R_p}}{e^{\frac{V_{oc}(a_G, T)}{mT}} - 1} \tag{44}$$

In turn,  $V_{oc}(1,T)$  and  $V_{oc}(0.2,T)$  can be calculated by:

$$V_{oc} = V_{oc,ref} + mT \ln\left(\frac{G}{G_{ref}}\right) + \mu_{Voc}(T - T_{ref}) \tag{45}$$

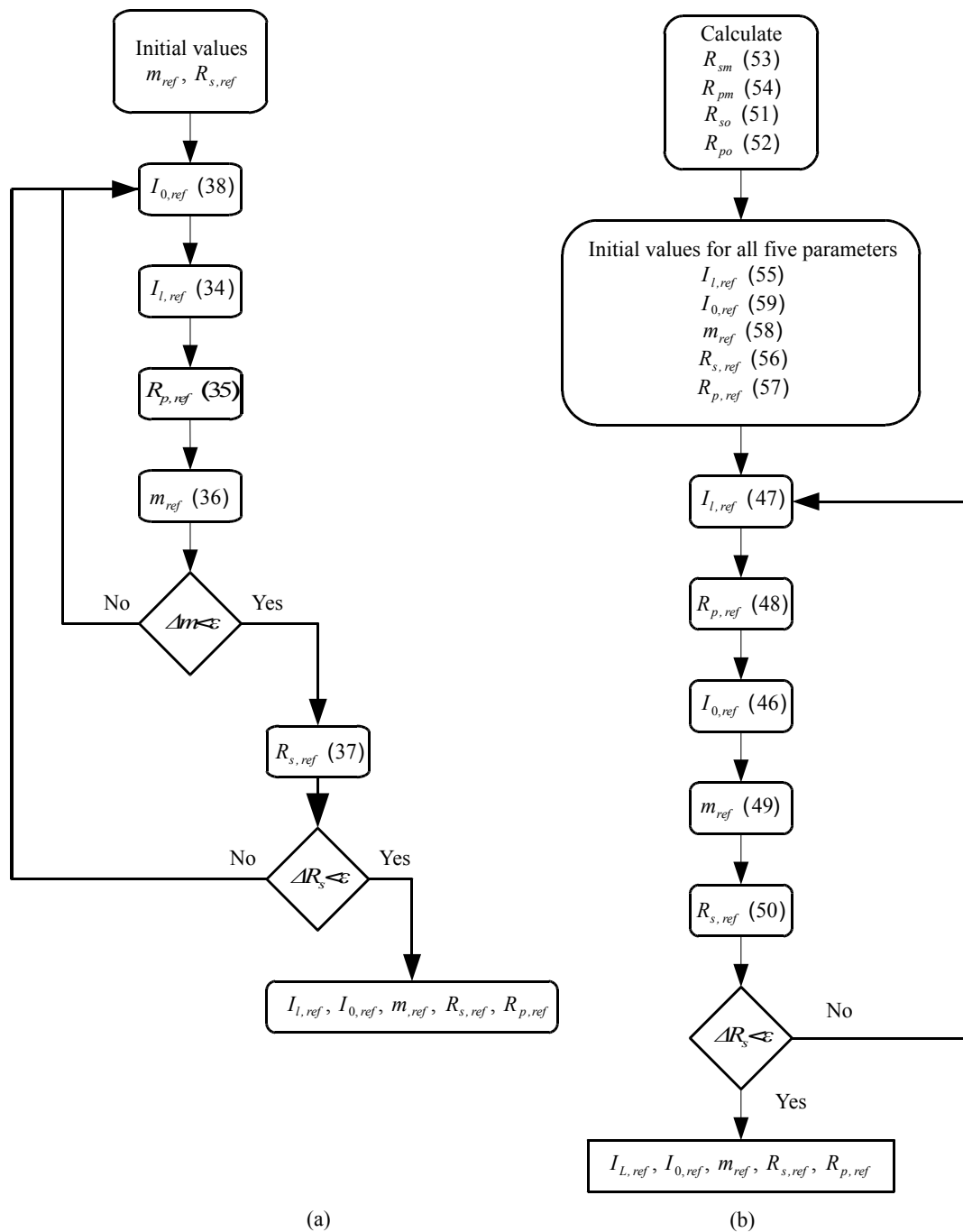


Figure 3. Flow charts of the proposed V. Lo Brano et al. (a) and M. Paulescu et al. (b) algorithms for calculating the five parameters at STC [11].

2.3 M. Paulescu et al.

In the case of the M. Paulescu et al. methodology, (5) is used to simulate the electrical behavior of a single photovoltaic cell [11]. The process also involves the calculation of the five parameters under STC and non-STC conditions, however the specifics vary.

2.3.1 Five parameters at STC

The system of proposed equations is readily provided at [11]. Each of (46-50) is an implicit expression of a single parameter:

$$I_{0,ref} = \frac{I_{l,ref} - I_{mp,ref} - \frac{V_{mp,ref} + I_{mp,ref}R_{s,ref}}{R_{p,ref}}}{e^{\frac{V_{mp,ref} + I_{mp,ref}R_{s,ref}}{m_{ref}V_{T,ref}}} - 1} \tag{46}$$

$$I_{l,ref} = I_{sc,ref} + I_{0,ref} \left[ e^{\frac{I_{sc,ref}R_{s,ref}}{m_{ref}V_{T,ref}}} - 1 \right] + \frac{I_{sc,ref}R_{s,ref}}{R_{p,ref}} \tag{47}$$

$$R_{p,ref} = \frac{R_{po} - R_{s,ref}}{1 - (R_{po} - R_{s,ref}) \frac{I_{0,ref}}{m_{ref}V_{T,ref}} e^{\frac{I_{sc,ref}R_{s,ref}}{m_{ref}V_{T,ref}}}} \tag{48}$$

$$m_{ref} = \frac{V_{oc,ref}}{V_{T,ref} \ln \left( \frac{I_{l,ref} + I_{0,ref} - \frac{V_{oc,ref}}{R_{p,ref}}}{I_{0,ref}} \right)} \tag{49}$$

$$R_{s,ref} = R_{so} - \frac{1}{\frac{I_{0,ref}}{m_{ref}V_{T,ref}} e^{\frac{V_{oc,ref}}{m_{ref}V_{T,ref}}} + \frac{1}{R_{p,ref}}} \tag{50}$$

The values of the series resistance at the open circuit point,  $R_{so}$ , and of the parallel resistance at the short circuit point,  $R_{po}$ , can be extracted from the following:

$$R_{so} = 0.002102 + 0.318070R_{sm} \tag{51}$$

$$R_{po} = -0.051914 + 2.505219R_{pm} \tag{52}$$

Equations (51) and (52) were empirically devised using data from various PV modules [11].  $R_{sm}$ ,  $R_{pm}$  are the series and parallel resistance at the maximum power point. They can be calculated in turn by the following equations:

$$R_{sm} = \frac{V_{oc,ref} - V_{mp,ref}}{I_{mp,ref}} \tag{53}$$

$$R_{pm} = \frac{V_{mp,ref}}{I_{sc,ref} - I_{mp,ref}} \tag{54}$$

According to the M. Paulescu et al. methodology, after giving specific initial values for all five parameters, the parameters are re-calculated through (46-50). The process is repeated until convergence of  $R_s$  is achieved. The proposed algorithm is the result of extensive numerical experiments during which, the fact that  $R_s$  had the slowest convergence rate was observed. Its flow chart is depicted on Figure 3 (b). The initial values of the parameters under reference conditions are calculated thusly:

$$I_{l,ref} = I_{sc,ref} \quad (55)$$

$$R_{s,ref} = R_{so} \quad (56)$$

$$R_{p,ref} = R_{po} \quad (57)$$

$$m_{ref} = 1 \quad (58)$$

$$I_{0,ref} = \frac{I_{l,ref} - I_{mp,ref} - \frac{V_{mp,ref} + I_{mp,ref} R_{s,ref}}{R_{p,ref}}}{e^{\frac{V_{mp,ref} + I_{mp,ref} R_{s,ref}}{m_{ref} V_T}} - 1} \quad (59)$$

Applying the above process, the values of the five parameters at STC are obtained:

$$I_{l,ref} = 8.1052 [A]$$

$$I_{0,ref} = 8.0740 \cdot 10^{-9} [A]$$

$$m_{ref} = 1.1442 \left[ \frac{V}{K} \right]$$

$$R_{s,ref} = 0.0042 [\Omega]$$

$$R_{p,ref} = 2.2757 [\Omega]$$

### 2.3.2 Five parameters outside STC

Having the reference values of the five parameters, the equations for dependence on reference conditions proposed at [9] can be used.

#### 2.4 E. Batzelis et al.

In [12], E. Batzelis and S. A. Papathanassiou developed a set of analytical expressions for the calculation of the five parameters at any operating conditions. This approach is based on the recently determined relationship between the modified ideality factor and the open circuit voltage and is characterized by robustness and easy of use. The implicit and explicit form of the equation that describes the model follow:

$$I = I_l - I_0 \left( e^{\frac{V + IR_s}{a}} - 1 \right) - \frac{V + IR_s}{R_p} \quad (60)$$

$$V = R_p (I_l + I_0) - (R_s + R_p) I - a W \left\{ \frac{I_0 R_p}{a} e^{\frac{R_p (I_l + I_0 - I)}{a}} \right\} \quad (61)$$

where  $W\{\}$  is the Lambert W function.  $W\{\}$  can be calculated using either a relevant programming or mathematical application or by using the following proposed approximation [12]:

$$W\{x\} = \ln(x) \left[ 1 - \frac{\ln(\ln(x))}{\ln(x) + 1} \right] \quad (62)$$

which provides an acceptable accuracy for  $x \geq 2$ .

2.4.1 Five parameters at STC

The proposed set of equations for the extraction of the reference parameters is:

$$a_{ref} = \delta_{ref} V_{oc,ref} \tag{63}$$

$$R_{s,ref} = \frac{[a_{ref}(w_{ref} - 1) - V_{mp,ref}]}{I_{mp,ref}} \tag{64}$$

$$R_{p,ref} = \frac{a_{ref}(w_{ref} - 1)}{\left[ I_{sc,ref} \left( 1 - \frac{1}{w_{ref}} \right) - I_{mp,ref} \right]} \tag{65}$$

$$I_{l,ref} = \left( 1 + \frac{R_{s,ref}}{R_{p,ref}} \right) I_{sc,ref} \tag{66}$$

$$I_{0,ref} = I_{l,ref} e^{-\frac{1}{\delta_{ref}}} \tag{67}$$

The parameter  $\delta_{ref}$  is determined by (68), while the auxiliary term  $w_{ref}$  by (69):

$$\delta_{ref} = \frac{a_{ref}}{V_{oc,ref}} = \frac{1 - 298.15\mu_{Voc}}{50.1 - 298.15\mu_{Isc}} \tag{68}$$

$$w_{ref} = W \left\{ e^{\frac{1}{\delta_{ref}} + 1} \right\} \tag{69}$$

Implementing the above process, yields the following values:

$$I_{l,ref} = 8.1344 [A]$$

$$I_{0,ref} = 1.1297 \cdot 10^{-10} [A]$$

$$a_{ref} = 1.1680 [V]$$

$$R_{s,ref} = 0.2608 [\Omega]$$

$$R_{p,ref} = 47.5206 [\Omega]$$

2.4.2 Five parameters outside STC

According to [12], the set of equations (63-67) are in effect for any operating conditions. Parameter  $\delta$  outside STC is expressed by:

$$\delta = \frac{a}{V_{oc}} = \frac{\frac{a_{ref} T}{T_{ref}}}{V_{oc}} = \delta_{ref} \frac{V_{oc,ref}}{V_{oc}} \frac{T}{T_{ref}} \tag{70}$$

Auxiliary term  $w$  is evaluated by:

$$w = W \left\{ e^{\frac{1}{\delta} + 1} \right\} \tag{71}$$

It is quite evident that, for this approach the short circuit, open circuit and maximum power points must be known in order to be applicable since, the values of  $V_{oc}$ ,  $I_{sc}$  and  $(V_{mp}, I_{mp})$  are required.

### 2.5 Calculation of power

With the I-V characteristic equation and its parameters under non-STC conditions, the operating current and voltage can be calculated for a specific connected load. In the present paper a purely resistive load with resistance  $R_L=10 \Omega$  was chosen. Its characteristic equation is:

$$I = \frac{V}{R_L} \quad (72)$$

The operating point (V,I) lies at the intersection of the characteristic equations of the module and the load. The substitution of (72) in the module's characteristic results in a non-linear equation that was solved using the Newton-Raphson open iterative method [21, 22]. The acquisition of the operating point (V,I) enables the calculation of the produced power by the simple formula:

$$P = VI \quad (73)$$

It should be noted that in the case of the M. Paulescu et al. methodology, the characteristic equation describes the solar cell. Assuming that all of the module's cells are identical and operate under the same conditions, the relationship of voltage and current between cell and module are given by [26]:

$$I_{mod} = I_{cell} N_p \quad (74)$$

$$V_{mod} = V_{cell} N_s \quad (75)$$

### 2.6 Newton-Raphson method

In all cases, the non-linear I-V characteristic was solved using the Newton-Raphson method [21, 22]. Newton-Raphson is an open iterative method meaning that, it only requires an initial value that is reasonably close to the root. Open methods, compared to bracketing methods, display faster convergence rate but, at the same time, have a chance to diverge or fluctuate around the solution. A major downside of this particular method is that it demands the knowledge of the derivative, a process that sometimes is difficult for complex functions.

According to the method, starting from an initial guess, a better approximation can be achieved from the following recursive formula:

$$x_i = x_{i-1} - \frac{f(x_{i-1})}{f'(x_{i-1})} \quad (76)$$

This process is repeated until the convergence criterion is satisfied:

$$|x_i - x_{i-1}| < \varepsilon \quad (77)$$

where  $\varepsilon$  is the error tolerance. A graphical representation of (76) can be seen in Figure 4.

It is apparent that for every approximation  $x_{i-1}$ , a better one ( $x_i$ ) of the actual solution  $x_r$  can be achieved through (76).  $x_i$  is at the intersection of the function's tangent at  $x_{i-1}$  and axis x.

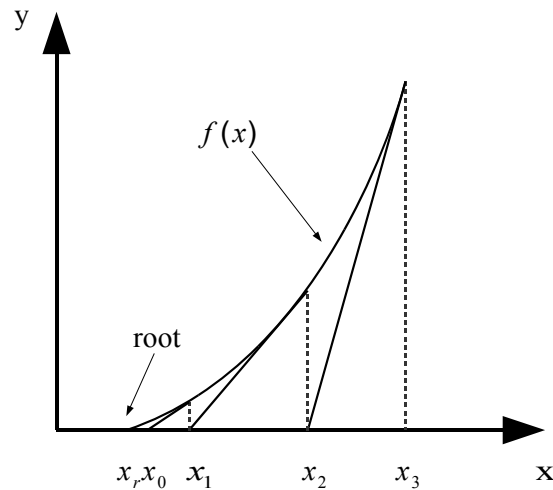


Figure 4. Graphical explanation of the Newton-Raphson method [22].

### 3. Results

It is a well known fact that high operating cell temperatures have a negative effect in a photovoltaic module's capacity to generate power [1, 27]. The possibility of using phase change materials as a thermal control medium has been explored and the conclusion was that phase change materials can be extremely effective in very specific ranges of temperature. Phase change materials that operate for prolonged periods of time in temperatures higher than their melting temperature combined with their inherent low heat conductivity behave as insulators, effectively increasing the cell temperature [28]. In [28] the cell temperature was calculated for four different cases:

- PV module.
- System of PV module in direct contact with RT20.
- System of PV module in direct contact with RT27.
- System of PV module in direct contact with SP25A8.

It was concluded that RT27 was the most effective. The cell temperature and insolation distributions for three periods of time were provided as input to the five-parameter model and their plots over time are depicted in Figures 5-7.

As far as the selection of the appropriate methodology for calculation of the generated power is concerned, while the De Soto et al. approach is the most cited, it requires the solution of a non-linear system. The initialization and convergence problems lead to the investigation of other alternatives (V. Lo Brano et al., M. Paulescu et al., E. Batzelis et al.). A comparative plot of the I-V characteristic curves at STC from the three methodologies is depicted in Figure 8. It is evident that the resulting I-V curves are almost coincidental. The methodology that was chosen for the calculation of the five parameters under non-reference conditions was the M. Paulescu et al. since it requires the least amount of manufacturer data, while its iterative algorithm is robust and free of initialization and convergence issues. The V. Lo Brano et al. requires data (temperature coefficients) that are sometimes not available. In addition, the initial inadequate graphical estimation of  $R_{so}$  and  $R_{po}$  may not always lead to convergence. This fact was experienced by the writers as several estimations of their values had to take place. The E. Batzelis et al. is a highly convenient approach, since it provides straight-forward analytical expressions. A disadvantage, that counter-balances its ease of implementation is that it requires the knowledge of the short circuit, open circuit and maximum power points at each operating condition.

The generated power in the case of the photovoltaic module as a unit and as a system in direct contact with RT27 is depicted in Figures 9-11. In the first period, power gain is small. Naturally, the benefit in terms of power is greater in the second period, since the air temperature is closer to RT27's operating temperature range (22-31 °C) [28]. During the third period, as the air temperature and insolation rise, the phase change material's low heat conductivity has an adverse effect on the cell temperature that consequently leads to a decrease in the generated power.

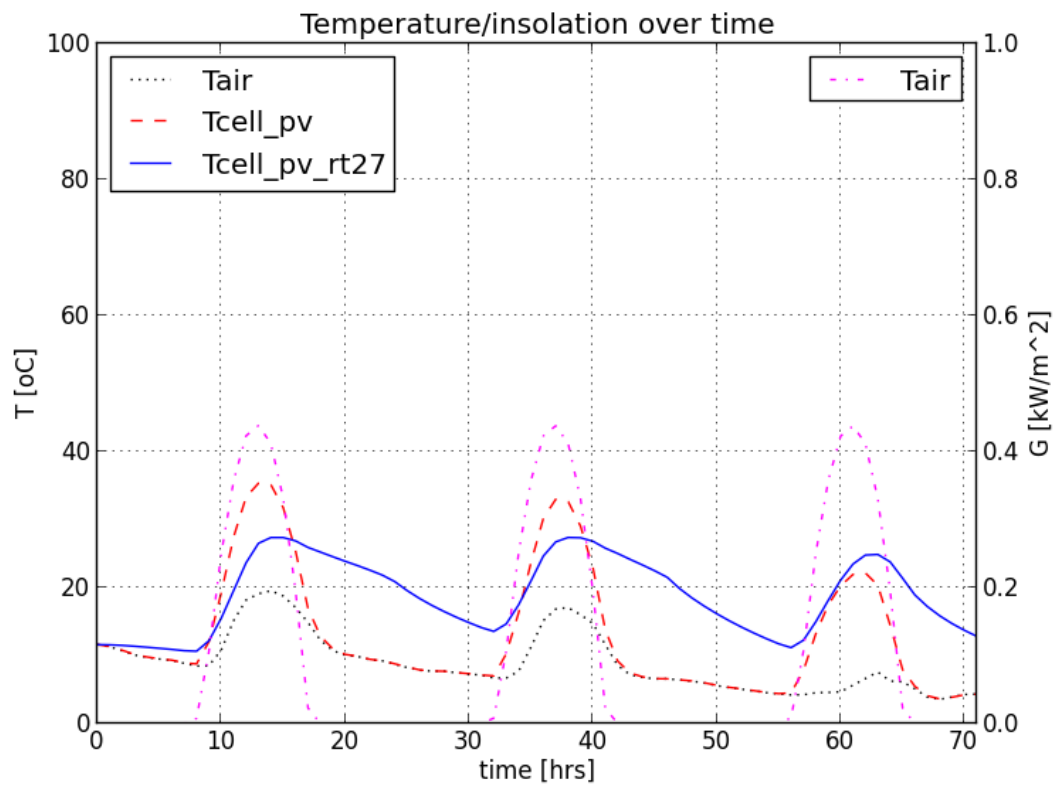


Figure 5. Solar cell temperature and radiation over time, 1-3/1.

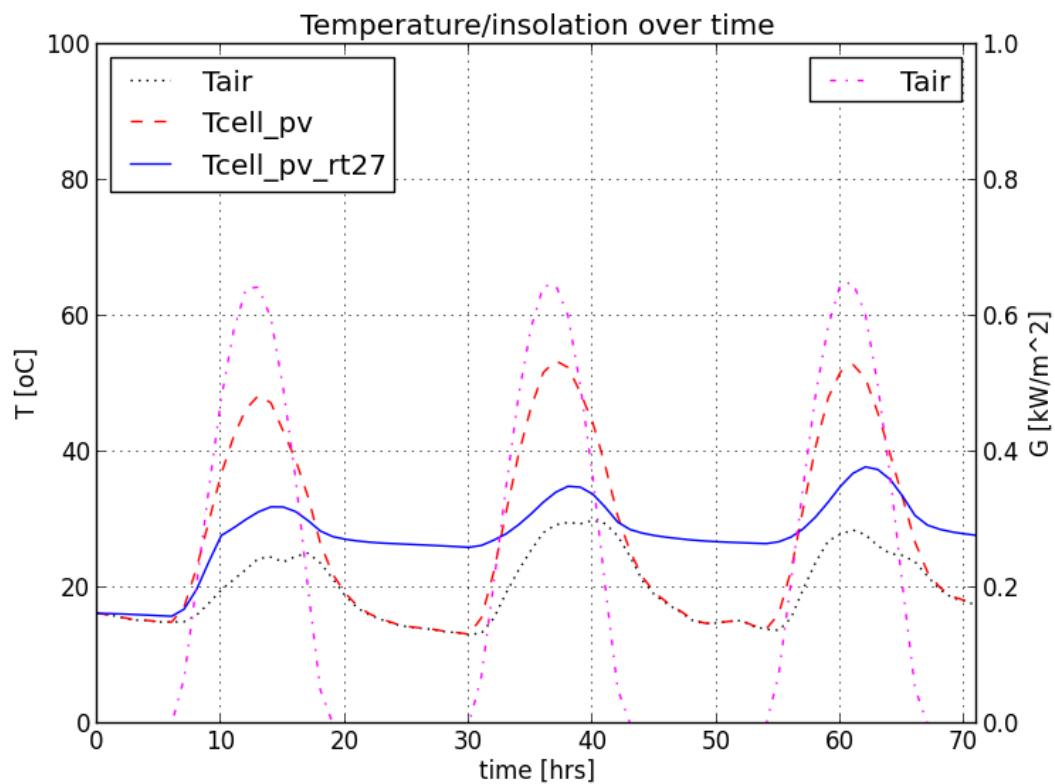


Figure 6. Solar cell temperature and radiation over time, 1-3/4.

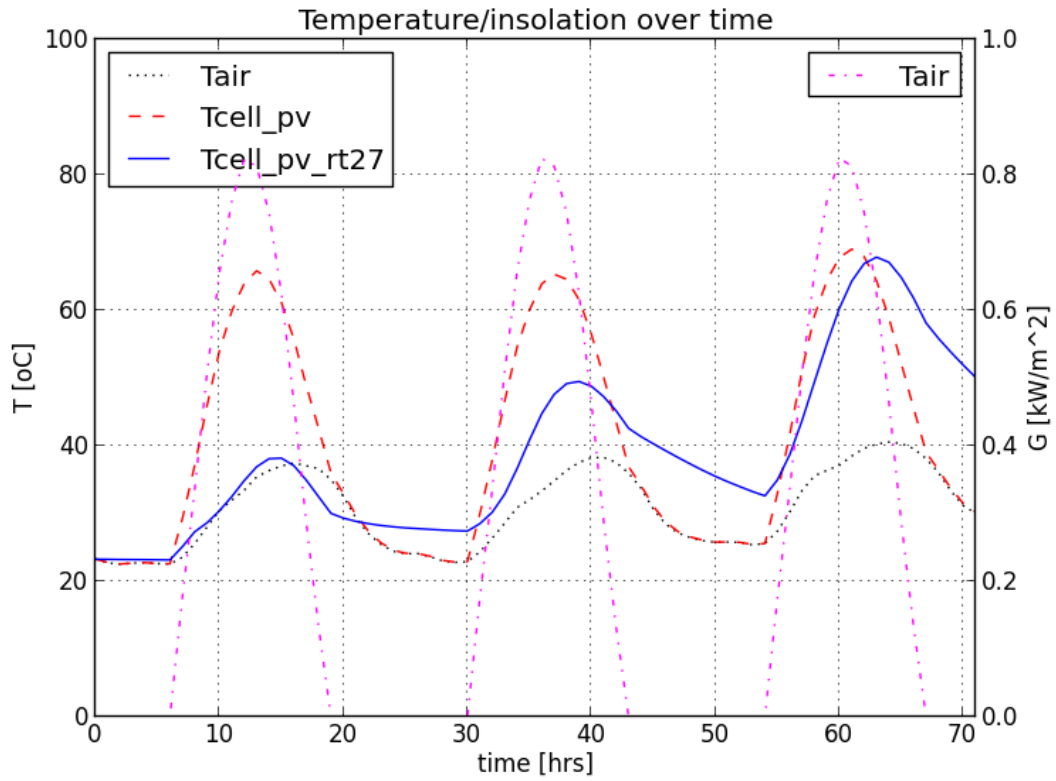


Figure 7. Solar cell temperature and radiation over time, 1-3/7.

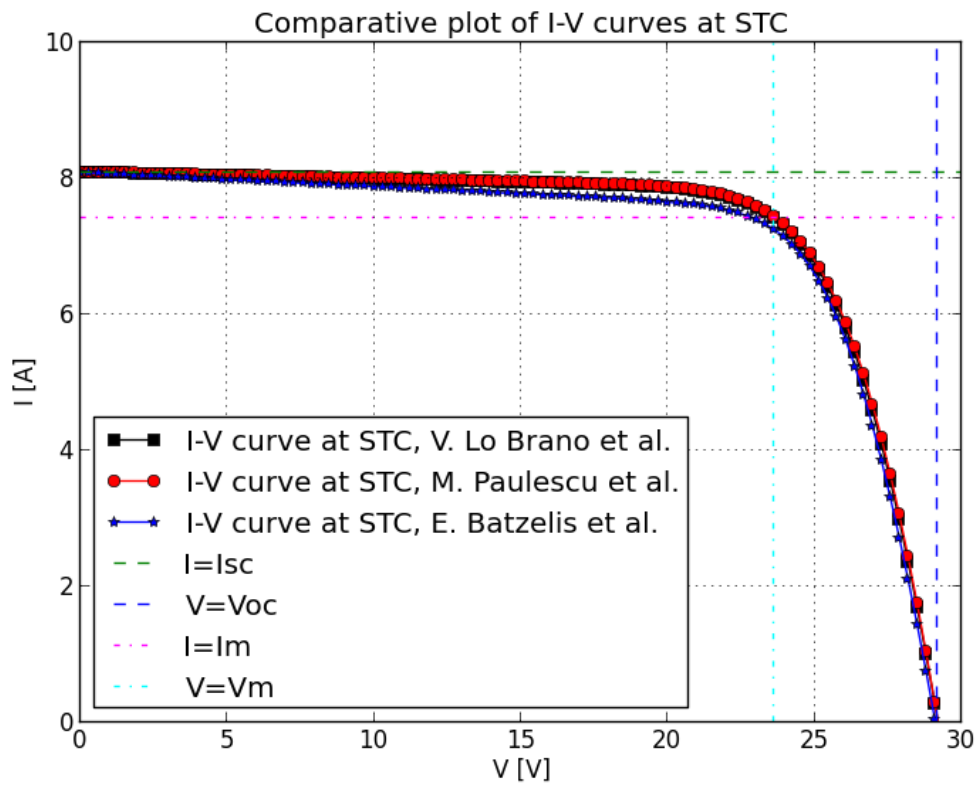


Figure 8. Comparative plot of the I-V curves at STC.



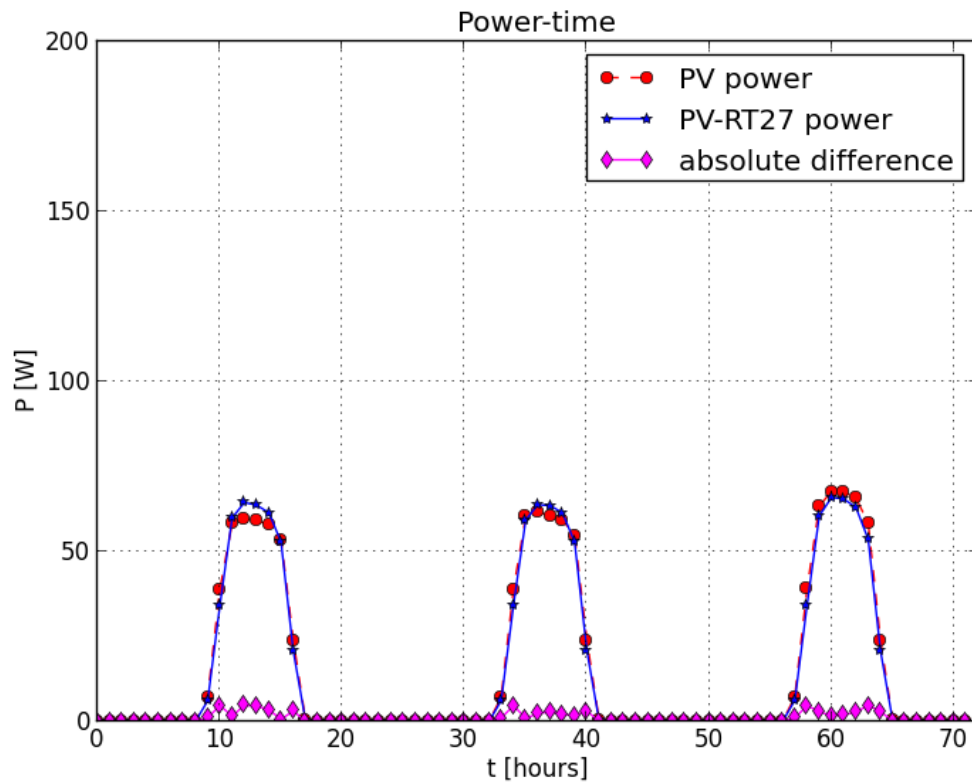


Figure 9. Comparative plot of generated power, 1-3/1.

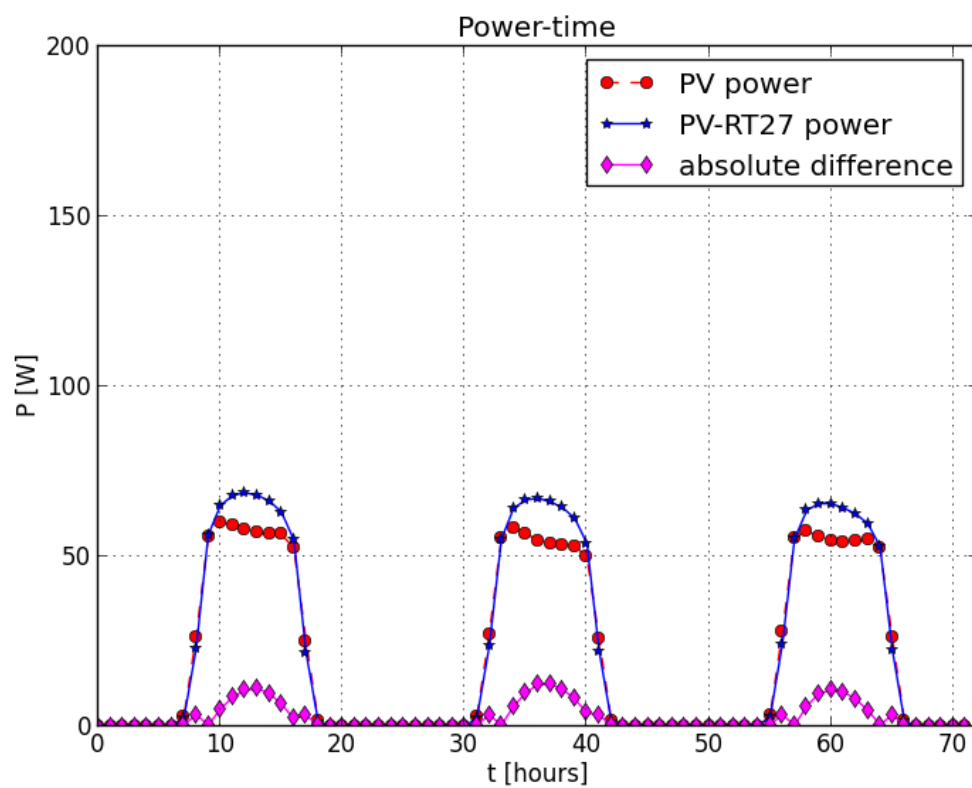


Figure 10. Comparative plot of generated power, 1-3/4.

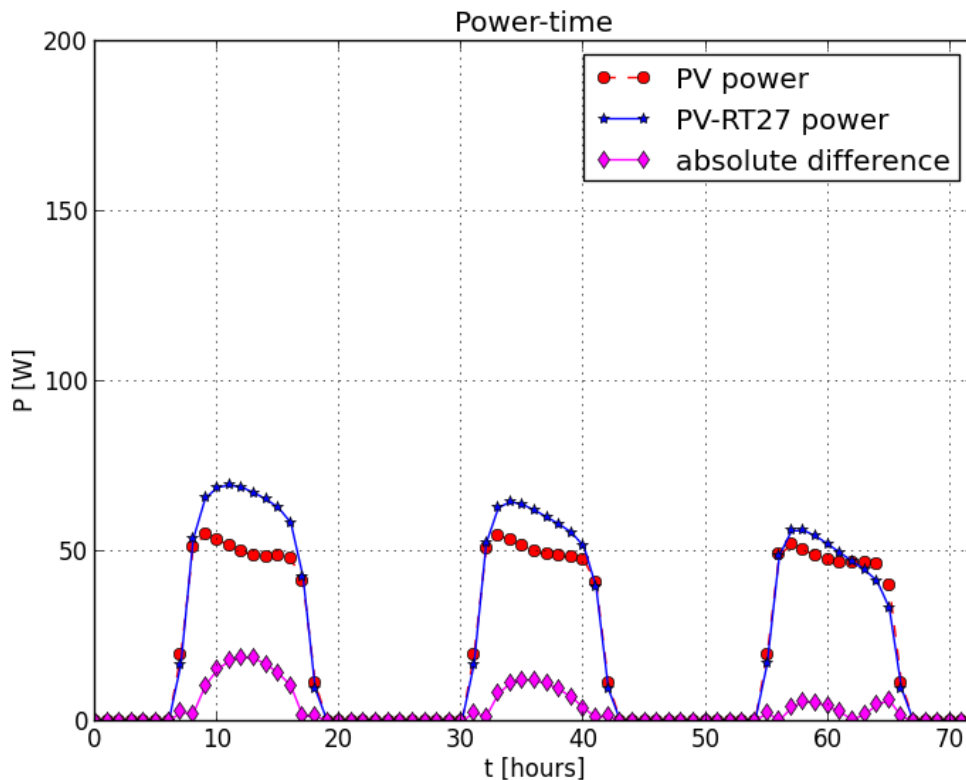


Figure 11. Comparative plot of generated power, 1-3/7.

#### 4. Conclusion

According to the resulting Figures 5-7 and 9-11, there is a direct correlation between cell temperature and generated power. The gain in power increases as the cell temperature drops. Evidently, the use of a PCM proves to be quite efficient for air temperatures close the PCM's temperature range. The figures of the third period of time (Figures 7 and 11) highlight a disconcerting fact: PCMs that operate for prolonged periods of time under temperatures higher than their melting behave as insulators. Their low thermal conductivity inhibits the rate with which they expel stored heat.

Suggestions for improvement:

- Taking an MPPT controller (Maximum Power Point Tracking) into consideration. A MPPT controller is a device that ensures that the photovoltaic module operates always on Maximum Power Point by adjusting the resistance of the connected load [9, 14, 15, 27].
- Taking advantage of the PCM's stored heat for heating or other purposes.
- Examine potential ways to increase the PCM's low thermal conductivity and assess their impact on the generated photovoltaic power. Among the suggested methods are the insertion of metal grids, the use of metal fins and forced convection (e.g. fans).

#### Nomenclature

*Latin characters*

AM: air mass at STC [-]

G: solar radiation [ $\text{kW/m}^2$ ]

I: current [A]

$I_0$ : reverse saturation current [A]

$I_D$ : diode current [A]

$I_L$ : photocurrent [A]

$I_{mp}$ : maximum power point current [A]

$I_{mod}$ : module current [A]

$I_{sc}$ : short circuit current [A]

K: thermal correction factor [ $\Omega/^\circ\text{C}$ ]

$k_B$ : Boltzmann constant [ $1.38064852 \cdot 10^{-23}$  J/K]

m: diode ideality factor [V/K]

$N_p$ : number of parallel solar cells [-]

$N_s$ : number of solar cells connected in series [-]

P: module power [W]

q: electron charge [ $1.602176565 \cdot 10^{-19}$  C]

$R_L$ : load resistance [ $\Omega$ ]

$R_s$ : series resistance [ $\Omega$ ]

$R_{sm}$ : series resistance at maximum power point [ $\Omega$ ]

$R_{so}$ : series resistance at open circuit point [ $\Omega$ ]

$R_p$ : parallel resistance [ $\Omega$ ]

$R_{pm}$ : parallel resistance at maximum power point [ $\Omega$ ]

$R_{po}$ : parallel resistance at short circuit point [ $\Omega$ ]

$T$ : cell temperature [ $^{\circ}\text{C}$ ]

$V$ : voltage [V]

$V_{mp}$ : maximum power point voltage [V]

$V_{mod}$ : photovoltaic module voltage [V]

$V_{oc}$ : open circuit voltage [V]

$V_T$ : thermal voltage [V]

$W\{\}$ : Lambert W function [-]

$w$ : auxiliary parameter related to  $\delta$  through

$$w = W\left\{e^{\frac{1}{\delta}+1}\right\} [-]$$

*Greek characters*

$\alpha$  [V]: modified diode ideality factor

$\alpha_G$ : ratio between actual solar radiation and solar radiation at STC [-]

$\delta$ : coefficient for the one-diode model, defined as the ratio of  $\alpha$  over  $V_{oc}$  [-]

$\mu_{isc}$ : short circuit temperature coefficient [ $\text{A}/^{\circ}\text{C}$ ]

$\mu_{Voc}$ : open circuit temperature coefficient [ $\text{V}/^{\circ}\text{C}$ ]

*Indices*

ref: STC/reference conditions

mod: photovoltaic module values

cell: solar cell value

## References

- [1] Mertens K. Photovoltaics. Fundamentals, technology and practice. John Wiley & Sons, 2014.
- [2] Khanna, V., Das, B. K., Bisht, D., Vandana, Singh, P. K. A three diode model for industrial solar cells and estimation of solar cell parameters using PSO algorithm. Renewable Energy 78 (2015) 105-113.
- [3] Chen, X., Yu, K., Du, W., Zhao, W., Liu, G. Parameters identification of solar cell models using generalized oppositional teaching learning based optimization. Energy 99 (2016) 170-180.
- [4] Krismadinata, Ping, N. A. R. H. W., Selvaraj, J. Photovoltaic module modeling using simulink/matlab. Procedia Environmental Sciences 17 (2013) 537-546.
- [5] Yildiran, N., Tacer, E. Identification of photovoltaic cell single diode discrete model parameters based on datasheet values. Solar Energy 127 (2016) 175-183.
- [6] Orioli, A., Di Gangi, A. A procedure to calculate the five-parameter model of crystalline silicon photovoltaic modules on the basis of the tabular performance data. Applied Energy (2013) 1160-1177.
- [7] Khalid, M. S., Abido, M. A. A novel and accurate photovoltaic simulator based on seven-parameter model. Electric Power Systems Research 116 (2014) 243-251.
- [8] Celik, A. N., Acikgoz, N. Modeling and experimental verification of the operating current of mono-crystalline photovoltaic modules using four- and five-parameter models. Applied Energy 84 (2007) 1-15.
- [9] De Soto, W., Klein, S. A., Beckman, W. A. Improvement and validation of a model for photovoltaic array performance. Solar Energy 80 (2006) 78-88.
- [10] Lo Brano, V., Orioli, A., Ciulla, G., Di Gangi, A. An improved five-parameter model for photovoltaic modules. Solar Energy Materials & Solar Cells 94 (2010) 1358-1370.
- [11] Paulescu, M., Mares, O., Badescu, V. A simple but accurate procedure for solving the five-parameter model. Energy Conversion and Management 105 (2015) 139-148.
- [12] Batzelis, E. I., Papathanassiou, S. A. A method for the analytical extraction of the single diode PV model parameters. IEEE Transactions of sustainable energy, Vol. 7, No. 2, April 2016.
- [13] Duffie, J. A., Beckman, W. A. Solar engineering of thermal processes. John Wiley & Sons, 1991.
- [14] Habberlin, H. Photovoltaics. System design and practice. John Wiley & Sons, 2012.
- [15] Luque, A., Hegedus, S. Handbook of photovoltaic science and engineering. John Wiley & Sons, 2011.
- [16] Bellia, H., Youcef, R., Fatima, M. A detailed modeling of photovoltaic module using MATLAB. NRIAG Journal of Astronomy and Geophysics (2014) 3, 53-61.
- [17] Steadman, J. W. Section III-Electronics." in R. C. Dorf, The Electrical Engineering Handbook. CRC Press, 1993.
- [18] Ghani, F., Rosengarten, G., Duke, M., Carson, J. K. The numerical calculation of single-diode solar-cell modeling parameters. Renewable Energy 72 (2014) 105-112.
- [19] Papadopoulos, E. Introduction to electrical circuits and systems. National Technical University of Athens Publishing, School of Mechanical Engineering, 2000.

- [20] Batzelis, E. I. PV string performance model using Lambert-W function and study of shading impacts. M. S. thesis, National Technical University of Athens, School of Electrical Engineering, 2012.
- [21] Kiusalaas, J. Numerical methods in engineering with Python 3. Cambridge University press, 2013.
- [22] Giannakoglou, K. X., Anagnostopoulos, I., Mpergeles, G. Numerical analysis for engineers. National Technical University of Athens Publishing, School of Mechanical Engineering, 2003.
- [23] Kyocera: KC175GHT specifications. Retrieved from: <http://www.kyocerasolar.com/assets/001/5191.pdf>
- [24] Kazmerski, L. L. Photovoltaics: A review of cell and module technologies. Renewable and sustainable energy reviews. Vol. 1, Nos 1/2, pp. 71-170, 1997.
- [25] De Soto, W. Improvement and validation of a model for photovoltaic array performance. M. S. thesis. University of Wisconsin-Madison, 2004.
- [26] Paulescu M et al., New procedure and field tests to assess photovoltaic module performance, Energy (2014). Retrieved from: <http://dx.doi.org/10.1016/j.energy.2014.03.085>
- [27] Plante, R. H. Solar energy. Photovoltaics and domestic hot water. Oxford: Elsevier science press, 2014.
- [28] Kladisios, P., Steggou-Sagia, A. Using phase change materials in photovoltaic systems for cell temperature reduction: A finite difference simulation method. Journal of Thermal Engineering Vol. 2, Special Issue 4, No.4, pp. 897-906, July 2016.



**Panagiotis Kladisios** received his MS degree in 2015 in Mechanical Engineering from the National Technical University of Athens. Currently, he is pursuing a Phd degree in heat transfer in the same university. His interests include, among others, solar systems, HVAC and phase change materials. He is the co-author of 1 article.  
E-mail address: [pkladisios@hotmail.gr](mailto:pkladisios@hotmail.gr)



**Athina Steggou-Sagia** Achaia, Greece. Mechanical Engineer. m. Nikolaos Sagias, 1 daughter. Education: Dipl. Mechanical Engineer, National Technical University of Athens, Greece, 1979; PhD, Thermodynamics, Properties and Phase Change of Refrigerant Mixtures, 1986. Appointments: Ministry of Public Works, 1980-81; Researcher, 1981-88, Lecturer, 1988-92, Assistant Professor, 1992-97, Associate Professor, 1997-2006, Professor 2006-today, National Technical University of Athens; Fellow, European Community; Experienced Researcher, Queen Mary and Westfield College, University of London, England, 1993-94. Publications: Numerous papers to international journals and international conferences; Books in Heat and Mass Transfer-Unit Operations. Memberships: Greek Technical Chamber, 1979-; Executive Council, Greek Association of Computational Mechanics, Athens, 1994-96, 1998-2000; National Technical University of Athens, The Senate, 2003-04. Address: 9 Iroon Polytechniou Str. Zografou, 15780 Athens, Greece.  
E-mail address: [asagia@central.ntua.gr](mailto:asagia@central.ntua.gr)